Water Research 182 (2020) 115950

Contents lists available at ScienceDirect

Water Research

journal homepage: www.elsevier.com/locate/watres

# Exploring the factors that influence the adsorption of anionic PFAS on conventional and emerging adsorbents in aquatic matrices

Congyue Wu [a], Max J. Klemes [b], Brittany Trang [b], William R. Dichtel [b, **], Damian E. Helbling [a, *]

[a] School of Civil and Environmental Engineering, Cornell University, Ithaca, NY, 14853, USA
[b] Department of Chemistry, Northwestern University, Evanston, IL, 60208, USA

ARTICLE INFO

*Article history:*
Received 31 January 2020
Received in revised form
10 April 2020
Accepted 14 May 2020
Available online 25 May 2020

*Keywords:*
PFAS
Cyclodextrin polymer
Activated carbon
Adsorption
Groundwater matrix
Adsorption inhibition

ABSTRACT

Per and polyfluoroalkyl substances (PFASs) have raised great concern due to their ubiquity in aquatic environments, and adsorption technologies are among the most promising treatment solutions. This study investigated the key factors that influence the adsorption of anionic PFASs on conventional and emerging adsorbents. Batch adsorption experiments were conducted to evaluate the removal of 20 target PFASs at environmentally relevant concentrations by three different activated carbon (AC) materials and two different β-cyclodextrin polymers (CDPs). Experiments were conducted in Milli-Q water and in groundwater. Major physical properties of the adsorbents were measured, along with general water chemistry parameters for each groundwater sample. Principal component analysis (PCA) was subsequently employed to extract the important associations from the multivariate dataset. The distinct performances of ACs and CDPs were attributed to their different surface chemistry and the distinct nature of their adsorption binding sites. Hydrophobic interactions dominated PFAS adsorption onto ACs while CDPs mostly attracted anionic PFASs via favorable electrostatic interactions. ACs of a smaller average particle size performed better, with our data pointing to an increased external specific surface area as the likely reason. *pH* and the concentration of *cations* were the primary contributors to adsorption inhibition in groundwater. Higher pH values limit anionic PFAS adsorption by deprotonating the functional groups on adsorbent surfaces. The elevated levels of *cations* in some groundwater samples limited the effects of attractive electrostatic interactions. Knowledge of PFAS adsorption mechanisms gained from this study can be used to design more efficient adsorbents and to predict their performance under a range of environmental scenarios.



## 1. Introduction

Per- and polyfluoroalkyl substances (PFASs) are anthropogenic compounds that were first introduced to the global market in the 1940s, and have been used as additives in food packaging, fabrics, carpets, nonstick cookware, paints, adhesives, electronics, personal care products, and firefighting foams (Guelfo et al., 2018; Schultes et al., 2019). Most perfluoroalkyl acids are present as anionic species in the environment, rendering them highly water soluble. One major pathway for human exposure to PFASs is the consumption of contaminated drinking water (Domingo and Nadal, 2019; Guelfo et al., 2018; Hatton et al., 2018; Martin et al., 2019). However, PFASs have such strong thermal, chemical, and biological stability that they are recalcitrant to most conventional drinking water treatment processes (Houtz et al., 2018; Merino et al., 2016). Adsorption of PFASs has been shown to be an effective removal technology, especially when applied to address real-world complexities (Arias Espana et al., 2015; Ateia et al., 2019; Klemes et al., 2019).

Activated carbons (ACs) are currently the most widely applied conventional adsorbents for PFAS removal from water. Granular ACs have been used to remove PFAS from water in packed-bed

*Abbreviations:* $pH_{pzc}$, point of zero charge of an adsorbent; ILIS, isotope-labeled internal standard; AC, activated carbon; CDP, β-cyclodextrin polymer; SUVA, specific UV absorbance; TOC, total organic carbon; HPLC, high-performance liquid chromatography; MS, quadrupole-orbitrap mass spectrometer; QC, quality control; LOQ, limit of quantification; PCA, principal component analysis.

* Corresponding author.
** Corresponding author.
*E-mail addresses:* wdichtel@northwestern.edu (W.R. Dichtel), damian.helbling@cornell.edu (D.E. Helbling).

https://doi.org/10.1016/j.watres.2020.115950
0043-1354/

filtration systems, though slow adsorption kinetics on granular ACs can lead to early breakthrough unless systems are designed with a significant excess of AC (Xiao et al., 2017b; Yu et al., 2009). Powdered ACs exhibit faster adsorption kinetics, but are more appropriately used in batch adsorption contactors that have lower water throughput (Hansen et al., 2010; Yu et al., 2009). In addition, the efficiency of granular and powdered ACs can be compromised by water matrix constituents including natural organic matter and inorganic ions, which leads to frequent regeneration or replacement of ACs (Inyang and Dickenson, 2017; Rahman et al., 2014). These deficiencies make ACs rather expensive options for remediation of PFAS-contaminated water.

β-Cyclodextrin polymers (CDPs) are emerging adsorbents that offer an alternative solution for remediation of PFAS-contaminated water. Previous research with CDPs has focused on the removal of perfluorooctanoic acid (PFOA) or perfluorooctane sulfonate (PFOS) from Milli-Q water (Karoyo and Wilson, 2013; Xiao et al., 2017a), though the efficacy of CDPs for removing broader groups of PFAS from groundwater has not been fully explored. More recently, we demonstrated that a novel CDP crosslinked with a reduced terephthalonitrile (referred to as amine-CDP, or aCDP, in this manuscript) exhibits high affinity for a set of ten anionic PFAS, with reported removal efficiencies of 80–98% in Milli-Q water (Klemes et al., 2019). However, no CDP has been evaluated for anionic PFAS removal in a real water matrix, and the effects of water matrix constituents on the performance of CDPs remain unknown.

This study was designed to help bridge these knowledge gaps and to specifically fulfill the following objectives: (1) evaluate the performance of conventional ACs and emerging CDPs to remove a wide range of PFASs from pure water and groundwater; (2) explore the physical properties of ACs that contribute to variable performance; and (3) explore the constituents of groundwater that influence the adsorption of anionic PFASs on each adsorbent. To meet the objectives, we first conducted batch adsorption experiments to evaluate the removal of 20 anionic PFASs at environmentally relevant concentrations by three conventional AC materials and two novel CDPs in Milli-Q water. The three best-performing adsorbents were subsequently selected to evaluate the removal of the target PFASs in spiked groundwater and in PFAS-contaminated groundwater. Various parameters describing the adsorbent characteristics and groundwater matrices were measured. Principal component analysis (PCA) was then employed to extract the important relationships from the multivariate dataset. The results of this study provide new insights on the factors that influence the adsorption of anionic PFAS on conventional and emerging adsorbents in aquatic matrices.

## 2. Materials and methods

### 2.1. PFAS stock solutions and reagents

We selected 20 PFASs as adsorbates for this study. These PFASs were selected to represent a set of anionic PFASs with varying hydrophobicity and types of hydrophilic head groups. Specifically, we selected nine perfluorocarboxylic acids (PFCAs), seven perfluorosulfonic acids (PFSAs), three fluorotelomer sulfonic acids (FTSs), and perfluoro-2-methyl-3-oxahexanoic acid (GenX). Stock solutions of each PFAS were prepared in appropriate solvents at a concentration of 1 g $L^{-1}$ or 50 mg $L^{-1}$, depending on the solubility of the PFAS. The stock solutions were then used to prepare an analytical mixture containing all 20 target PFASs, and an internal standard mixture containing 7 isotope-labeled internal standards (ILISs), both in Milli-Q water and at a concentration of 100 μg $L^{-1}$. The stock solutions and mixtures were stored at −20 °C and 4 °C, respectively, until usage. Details regarding the 20 PFASs, the 7 ILISs, and the solvents and reagents used in this study are provided in Tables S1 and S2 of the Supplementary Data (SD).

### 2.2. Adsorbent materials

We selected three activated carbon materials (ACs) and two β-cyclodextrin polymers (CDPs) as adsorbents for this study. These include the commercially available CCAC AquaCarb® (1230C, Westates Carbon, Siemens, Roseville, MN), AWAC Filtrasorb® (400-M, Calgon Carbon Co., Pittsburgh, PA), and CDP+ (DEXSORB + ™, CycloPure, Encinitas, CA); we note that the performance of CDP+ is reported here for the first time. We also acquired HFAC (granular activated carbon used at a local drinking water treatment facility to process PFAS-contaminated groundwater) and synthesized aCDP (amine-CDP) according to a previously described method (Klemes et al., 2019). Each AC was pulverized with a mortar and pestle and sieved into different particle size bins (10–75, 125–212, 425–850, and 1000–1700 μm); the two smaller size bins are representative of PAC and the two larger size bins are representative of GAC. All sieved ACs were stored in amber vials at room temperature until use in experiments. A detailed material characterization of the adsorbents, including measurements of the *particle size*, *total pore volume*, *micropore volume*, and *zeta-potential*, is provided in Table S3. The particle diameters were determined using U.S. standard sieves; the total pore and micropore volumes were measured with $N_2$ adsorption isotherms generated using a Micromeritics ASAP 2420; the zeta-potential values were measured at pH 7–8, using a Malvern Zetasizer Nano instrument with a He–Ne laser (633 nm, max 5 mW).

### 2.3. Groundwater sources and characterizations

We collected groundwater from two wells near military training sites in Pennsylvania, which we note as WA and AA in this study. Based on their background concentrations of PFCAs and PFSAs (Fig. S1), these groundwater samples were representative of PFAS-contaminated groundwater. Groundwater from a private well in New York (GW) was selected as the representative sample for uncontaminated groundwater and was used for spiked groundwater experiments. All groundwater samples were collected in 1L HDPE sampling bottles to minimize potential PFAS adsorption onto any surface, then sealed with parafilm and transported to our laboratory in Styrofoam coolers packed with frozen ice packs. Trizma base was used as a buffer and PFAS preservative during the collection of some of the samples. Specifically, groundwater samples WA-A, AA-A, GW-A were amended with Trizma to a final concentration of 5 g $L^{-1}$ (as instructed in EPA method 537.1) and groundwater sample WA-D was collected with no Trizma added. All samples were stored at 4 °C upon receipt, until usage. The groundwater samples were handled with polypropylene syringes and filtered through 0.22 μm PVDF filters (Restek) prior to any experiment or analysis. General water chemistry parameters were measured for all filtered groundwater samples, including: *pH*, *conductivity*, total organic carbon (*TOC*), specific UV absorbance (*SUVA*), and the concentrations of a variety of *cations* and *anions* ($K^+$, $Ca^{2+}$, $Na^+$, $Mg^{2+}$, $F^-$, $Cl^-$, $NO_3^-$, $SO_4^{2-}$, $PO_4^{3-}$). All parameters were measured using standard methods; further details and the resulting data are provided in Tables S4 and S5. All water chemistry analyses were conducted within 4 weeks of receiving a groundwater sample.

### 2.4. Rotator batch experiments

For spiked experiments, 10 mL of the water sample (Milli-Q or GW-A) was transferred into 15 mL polypropylene centrifuge tubes (Corning) and spiked with the 20 PFAS analytical mixture to a target concentration of 500 ng $L^{-1}$ (adsorbate concentration selected to

represent an environmentally relevant level). For unspiked experiments, 10 mL of the groundwater sample (WA-A, WA-D, or AA-A) was transferred into 15 mL centrifuge tubes with no spiking of any PFAS. The centrifuge tubes were then loaded onto a rotary tube revolver (Thermo Scientific) and rotated at 40 revolutions per minute (rpm) for over 20 h to provide a homogeneous solution. Adsorbents (ACs or CDPs) were then added into the centrifuge tubes at a dose of approximately 10–60 mg $L^{-1}$ (representing the economically feasible dose for drinking water treatment). The centrifuge tubes were then reloaded onto the tube revolver and rotated at 40 rpm for 48 h of treatment. Triplicate experiments with each adsorbent were conducted at 23 °C. The centrifuge tubes were sacrificed at predetermined time points (0.5, 4, 8, 24, 48 h), filtered with a 0.45 μm cellulose acetate filter (Restek), transferred into 18 mm screw top headspace vials (Fisher Scientific), spiked with the mixture of 7 ILISs, and stored at 4 °C until HPLC-MS analysis; we note that only limited PFAS adsorption was observed in recovery experiments with the 0.45 μm cellulose acetate filters. Control experiments were performed under the same conditions with no addition of adsorbents. We note that the pH of the groundwater experiments was sufficiently buffered to remain constant throughout the batch experiments; the pH of experiments in Milli-Q water was assumed to remain stable at around 6.7, as has been experimentally confirmed in similar types of batch adsorption experiments (Ling et al., 2020).

### 2.5. PFAS quantification

Quantification of 20 target PFASs in all prepared samples (spiked with ILISs) was conducted by means of high-performance liquid chromatography (HPLC) coupled with quadrupole-orbitrap mass spectrometery (MS, QExactive, ThermoFisher Scientific). Analytical information for all PFASs and their ILISs is provided in Table S6. Briefly, the mobile phase consisted of (A) LC-MS grade water amended with 20 mM ammonium acetate and (B) LC-MS grade methanol. Samples were injected at 5 mL volumes onto a Hypersil Gold dC18 12 μm 2.1 × 20 mm trap column (ThermoFisher Scientific) and were eluted onto an Atlantis® dC18 5 μm 2.1 × 150 mm analytical column (Waters) with a pump delivering 300 μL $min^{-1}$ of a mobile phase gradient starting at 40% B; the gradient composition followed that described in EPA method 537.1. The column temperature was held constant at 25 °C. The HPLC-MS was operated with electrospray ionization in negative polarity mode. Calibration standards (n = 8) were prepared in Milli-Q water with concentrations ranging between 0 ng $L^{-1}$ to 750 ng $L^{-1}$ for external calibration. Analytes were quantified from calibration standards (spiked with the same amount of ILIS) based on the PFAS target-to-ILIS peak area ratio responses by linear least-squares regression. Calibration curves were run at the beginning of the analytical sequence. Instrument blanks were run before and after the calibration curve and each batch of triplicate samples. One quality control (QC) sample was placed halfway through every analytical sequence to ensure minimal contamination and adequate MS performance (QC tolerance set at ±30%). Quality control and limits of quantification (LOQs) are provided in Tables S7 and S8.

### 2.6. Data analysis

The removal of each PFAS in each sample was calculated as described in **Equation (1)**:

$$Rmvl_{\,i,\ rep\,j} = \left(1 - \frac{c_{ij,t}}{c_{i,0}}\right) \times 100\% \qquad \text{Equation 1}$$

where $i$ is any of the 20 target PFASs; $j$ is the number of the replicate, $j = 1, 2, 3$; $t$ is the time point at which the sample was taken, $t = 0.5, 4, 8, 24, 48$ hr; $c_{ij,\,t}$ is the concentration of $i$ in replicate $j$ taken at $t$ hr; and $c_{i,\,0}$ is the concentration of $i$ in the "0 h" control sample. Then, the removal of each PFAS was calculated as the arithmetic average of three replicates.

To quantify the overall performance of each adsorbent, the weighted average removal of all 20 target PFASs was calculated at each time point based on **Equations 2** and **3**:

$$weight_i = \frac{c_{i,0}}{\sum c_{i,0}} \qquad \text{Equation 2}$$

$$weighted\ avg\ Rmvl = \sum (weight_{\,i} \times Rmvl_{\,i}) \qquad \text{Equation 3}$$

where $weight_i$ is the weight that $i$ carries in the calculation (based on its share of initial concentration in the matrix); and *weighted avg Rmvl* is the overall removal of all PFASs in the matrix (after considering the distinctions among initial concentrations).

To quantify the extent of adsorption inhibition for each adsorbent in the different groundwater matrices, we defined the parameter:

$$Matrix\ Effect = \frac{weighted\ avg\ Rmvl \text{ in GW}}{weighted\ avg\ Rmvl \text{ in Milli\_Q}} \qquad \text{Equation 4}$$

which quantifies how the adsorbent performs in a groundwater sample relative to Milli-Q water. The *Inhibition%* then provides a quantitative metric on how much the performance of an adsorbent is inhibited in a specific groundwater matrix relative to Milli-Q water.

$$Inhibition\% = (1 - Matrix\ Effect) \times 100\% \qquad \text{Equation 5}$$

Principal component analysis (PCA) is a statistical method that reduces the dimensionality of a multivariate dataset, and helps visualize the connections among observations and inter-correlated quantitative variables (Mostert et al., 2010; Pérez-Arribas et al., 2017). We used the *FactoMineR* and *factoextra* packages in the R Statistical Software to construct PCA-biplots that describe the relationships between adsorbent performance and the major physical properties of the adsorbents or the basic chemical parameters of the groundwater samples.

## 3. Results and discussion

### 3.1. PFAS removal by each adsorbent in Milli-Q water

The data provided in Fig. 1 show PFAS removal in Milli-Q water after 4 h of contact time on each of the five adsorbents (Fig. S2 shows removal at other contact times and Table S9 provides the average and standard deviation of the removal at each time point for all experiments). The three ACs are grouped into four particle size bins (10–75 μm, 125–212 μm, 425–850 μm, 1000–1700 μm) and the CDPs were evaluated in their as-synthesized particle sizes (212–425 μm for aCDP and <63 μm for CDP+). There is a clear difference in the performance of the ACs as a function of their particle size; ACs from the two larger size bins remove PFAS from Milli-Q water to a lower extent after 4 h of contact time than the ACs from the two smaller size bins, though greater extents of removal were observed after longer contact times (Fig. S2 and Table S9). This is consistent with previous studies that report slower and lower extents of PFAS adsorption on larger-sized ACs (Chen et al., 2017; Yu et al., 2009). It is widely known that the kinetics of adsorption on AC is controlled by relatively slow intra-

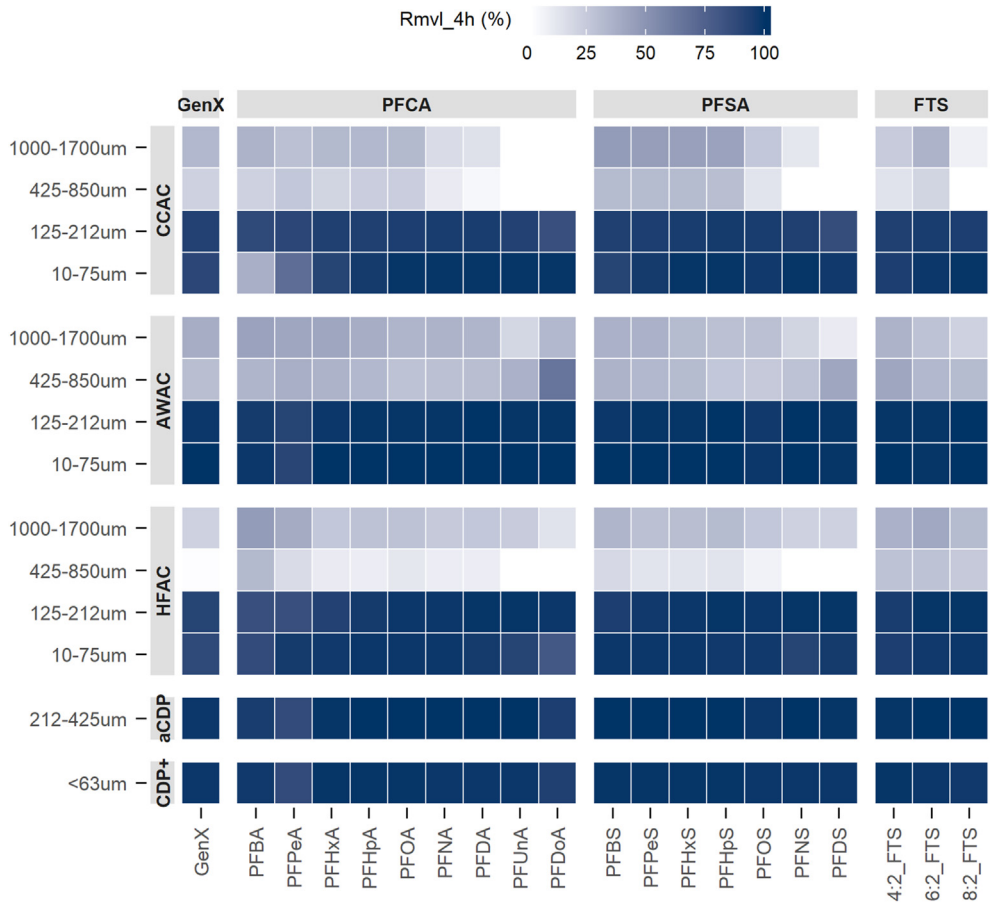


**Fig. 1.** Heatmap of 20 PFASs adsorption onto 5 adsorbents in Milli-Q water at 4h. The PFAS compounds were grouped by their corresponding classes and listed with increasing chain length within each group along the x-axis. The adsorbents were grouped by their corresponding types and listed with increasing particle size within each group along the y-axis. The tiles were colored according to the arithmetic average removal (calculated from Equation (1)) for each pair of the coordinates.

particle diffusion, which requires adsorbates to diffuse into micropores to access free surfaces. Micropores can also be blocked by larger adsorbates which may limit the capacity of AC adsorbents (Punyapalakul et al., 2013; Wang et al., 2019; Zhao et al., 2011). We attribute the relatively slow adsorption of anionic PFAS on larger-sized ACs to intra-particle diffusion limitations that become less important for smaller-sized ACs that have greater specific external surface area. It is also interesting to note that shorter-chain PFASs are removed from Milli-Q water to greater extents than longer-chain PFASs by larger-sized ACs, whereas longer-chain PFASs are removed to greater extents than shorter-chain PFASs by smaller-sized ACs. We also attribute this finding to the greater importance of intra-particle diffusion for larger-sized ACs and the more rapid diffusion of smaller PFAS.

ACs from the two smaller size bins (10–75 μm, 125–212 μm) remove nearly all of the PFAS from Milli-Q water after 4 h of contact time with the exception of the shorter-chain PFCAs (*i.e.*, PFBA, PFPeA); similar results on the removal of anionic PFAS on powdered ACs have been previously reported (Hansen et al., 2010; Punyapalakul et al., 2013; Wang et al., 2019). The enhanced performance of powdered ACs has previously been attributed to either the generation of more internal active binding sites during pulverization and the consequent shorter diffusion distances required to access them (Yu et al., 2009), or the increased specific external surface area of smaller-sized AC particles which can provide access to more binding sites even in the presence of larger adsorbates that block access to internal micropores (Ando et al., 2010; Partlan et al., 2016). Therefore, the smaller-sized ACs in this study exhibit more rapid PFAS adsorption kinetics and greater extents of adsorption than the larger-sized ACs.

The two CDPs also remove nearly all of the PFASs from Milli-Q water after 4 h of contact time. Both of the CDPs evaluated in this study consist of β-cyclodextrin monomers crosslinked with rigid aromatics containing weakly basic (aCDP) or permanently cationic (CDP+) functional groups. The interior cavity of the β-cyclodextrin monomer is the most likely active site for adsorption on CDPs, and the β-cyclodextrin monomer is known to encapsulate anionic PFASs to form well-defined host-guest complexes via hydrophobic interactions (Karoyo et al., 2011; Tang et al., 2019; Weiss-Errico and O'Shea, 2017; Xiao et al., 2017a). Additionally, the protonated crosslinkers of both CDPs may facilitate the transport of anionic PFASs to the β-cyclodextrin monomers or provide alternate adsorption sites through complementary electrostatic interactions (Nassi et al., 2014; Zhang et al., 2011b).

### 3.2. Physical properties that control PFAS adsorption on activated carbon

To further explore the adsorption behavior of anionic PFASs on ACs, we constructed a PCA-biplot that describes the relationships between PFAS removal performance and the major physical properties of the ACs in each of the twelve experiments (*i.e.*, three ACs, four size bins) conducted in Milli-Q water. The four physical properties considered in the PCA analysis were *particle size*, *total*

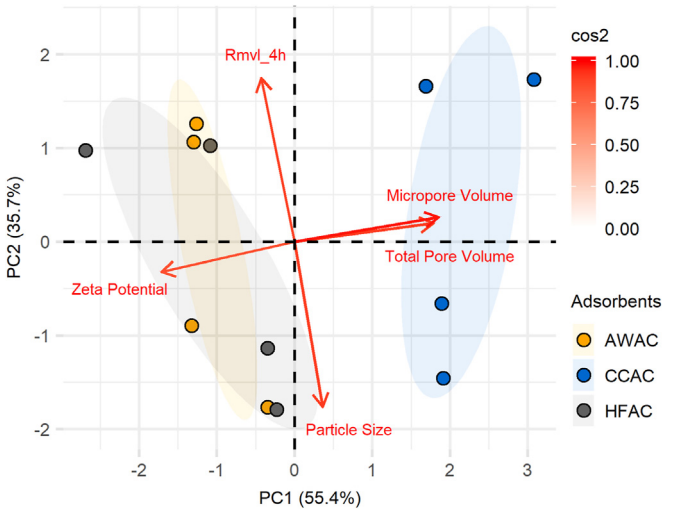


**Fig. 2.** PCA biplot demonstrating the correlations among four adsorbent properties of activated carbons and the weighted average removal of PFASs (calculated by Equation (3)) at 4h in Milli-Q water. The PCA was established based on a multi-dimensional dataset with 5 variables and 12 observations (four size bins by three types of activated carbon). The biplot was plotted against the first two primary components (i.e. PC1 and PC2), which combined to have explained more than 91% of the total variance in the original dataset. The observations were plotted as scattered points and were colored and grouped by their corresponding adsorbent types, and a 95% confidence ellipse was added for each group of adsorbent. The variables were plotted as straight arrows, and each variable was colored by its quality of representation (labeled as "cos2" in the legend) on the selected primary components (a lighter color indicates that the variable contributed less to the primary components). The correlations between variables were manifested by the angles in between the arrows. The magnitude an observation had for a certain variable was revealed by the point's position relative to the direction of the arrow (if the point locates in the same direction that an arrow is pointing at, the observation has a higher magnitude of this chosen variable). (For interpretation of the references to color in this figure legend, the reader is referred to the Web version of this article.)

*pore volume*, *micropore volume*, and *zeta-potential*. The results of the PCA analysis are provided as Fig. 2.

It is evident that, when considering PFAS adsorption on ACs in general, *particle size* is the leading factor to be considered. The *particle size* was determined as the average particle diameter of each size bin and a strong negative association was discovered between *particle size* and the weighted average PFAS removal at 4 h. This outcome is consistent with the qualitative findings described in Fig. 1; removal of anionic PFAS is enhanced with decreasing *particle size*. The *total pore volume* is the weight specific total pore volume of an adsorbent and is estimated from the $N_2$ adsorption isotherm. The *micropore volume* is the distribution of micropores in the adsorbent and is likewise calculated based on the $N_2$ adsorption measurements. As demonstrated in Fig. 2, neither of these properties associate with *particle size* or with the weighted average PFAS removal at 4 h (*Rmvl_4h*). This important finding excludes the likelihood that the improved performance of smaller-sized ACs is related to enlarged intra-particle pores, as proposed by a previous study (Piai et al., 2019). On the contrary, this finding corroborates several other studies that report that the BET surface area and pore volume distributions of ACs are not altered significantly during pulverization (Ando et al., 2010; Partlan et al., 2016). Therefore, the enhanced performance of smaller-sized ACs must be attributed to other mechanisms, such as an increased specific external surface area (Ando et al., 2010; Murray et al., 2019; Yu et al., 2009) or the generation of more active binding sites that were originally inaccessible (Ando et al., 2010). The *zeta potential* is used to represent the surface charge of each AC in the pH range of 7–8. This property also exhibited little association with the weighted average PFAS removal at 4 h, indicating that hydrophobic interactions dominate the adsorption of anionic PFAS on ACs.

### 3.3. PFAS removal by each adsorbent in groundwater

To examine how PFAS removal changes in natural groundwater matrices, further experiments were conducted with three of the adsorbents in groundwater: CDP+, aCDP, and AWAC (the adsorbents were selected based on their performance in Milli-Q water). We used AWAC from the 125–212 μm size bin to increase the validity and reliability of the comparison among different types of adsorbents with minimum impact from their particle size. The data provided in Fig. 3 show PFAS removal in groundwater matrices after 4 h of contact time on each of the three adsorbents (Fig. S3 shows removal at other contact times and Table S10 provides the average and standard deviation of the removal at each time point for all experiments). Note that GW-A was a pristine groundwater sample that was spiked with 500 ng $L^{-1}$ of PFAS and that the remaining groundwater samples were not spiked with PFAS and evaluated for removal of the native PFASs that were present in those samples; gray squares in Fig. 3 indicate that a PFAS was not present in a particular groundwater sample above the LOQ.

Overall, the extent of PFAS removal on all three adsorbents in groundwater was less than what was observed in Milli-Q water (Fig. 1), which can be attributed to matrix interferences caused by the chemical properties of each groundwater. Unlike the performance of larger-sized ACs in Milli-Q water, longer-chain PFAS were always removed to greater extents than shorter-chain PFAS by all adsorbents in the groundwater experiments. This is because adsorption of PFAS on CDPs and smaller-sized ACs is not controlled by intra-particle diffusion limitations that can favor the adsorption of smaller-sized adsorbates. Rather, the affinity of PFAS for the binding sites on each of the adsorbents is driven in part by hydrophobic interactions that are not diffusion-limited (Ahrens et al., 2010; Eschauzier et al., 2012; Inyang and Dickenson, 2017; Zhang et al., 2016). Therefore, longer-chain PFASs have a higher tendency to partition from the bulk solution to a solid surface.

The data in Fig. 3 also demonstrate that, for most PFASs and in most groundwater samples, the extent of PFAS removal is the greatest on CDP+. This suggests that the matrix interferes with adsorption on AWAC and aCDP more than it does for CDP+. To more accurately quantify the differences in performance of each adsorbent in each groundwater, we calculated the *Inhibition%* for each adsorbent in each groundwater as described in Equation (5). These data are presented in Fig. 4. The height of each bar in Fig. 4 represents the total extent to which PFAS removal was inhibited in each groundwater sample relative to Milli-Q water. These data demonstrate that the extent of PFAS adsorption on CDP+ was always inhibited the least compared to the other adsorbents, except in groundwater AA-A (Fig. 4b), implying that a particular constituent of groundwater AA-A might selectively inhibit the adsorption of anionic PFAS on CDP+. Further, the extent of PFAS adsorption on aCDP was always inhibited the most compared to the other adsorbents, except in groundwater WA-D (Fig. 4d), implying that a particular constituent of groundwater WA-D might enhance adsorption of anionic PFAS on aCDP.

The colors of the bars in Fig. 4 refer to the specific groups of PFAS included in this study (*i.e.*, PFCAs, PFSAs, FTSs, and GenX). Although the FTSs and GenX were not always present at quantifiable levels in the groundwater samples (Fig. 3 and Fig. S1), PFCAs and PFSAs were measured in every groundwater sample. Larger bars for a specific group of PFASs in Fig. 4 suggests that the extent of adsorption inhibition was greater for that group of PFASs in a particular groundwater sample. From these data, we can conclude that the extent of adsorption inhibition was significantly less for PFSAs than

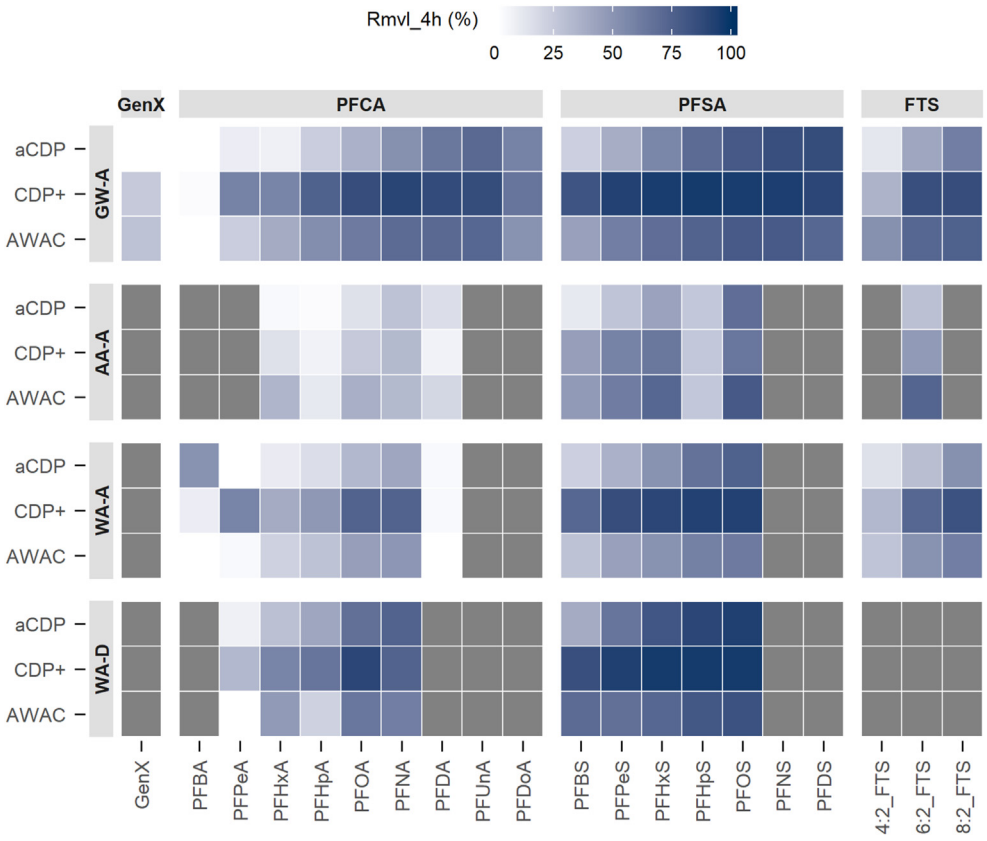


**Fig. 3.** Heatmap of 20 PFASs adsorption onto 5 adsorbents in groundwater matrices at 4 h. The PFAS compounds were grouped by their corresponding classes, and listed with increasing chain length within each group along the x-axis. The adsorbents were grouped by their corresponding types, and listed with increasing particle size within each group along the y-axis. The tiles were colored according to the arithmetic average removal (calculated from Equation (1)) for each pair of the coordinates (a gray tile represents that the corresponding PFAS compound had a level below our limit of quantification in the specific groundwater sample).

it was for PFCAs for all adsorbents; this is especially obvious in Fig. 4c and d where the removal of PFSAs was not inhibited at all. This observation is consistent with previous studies illustrating the relatively high adsorption affinity of PFSAs on a variety of adsorbents (McCleaf et al., 2017; Xiao et al., 2017b; Zhang et al., 2016).

### 3.4. Chemical parameters of groundwater that contribute to adsorption inhibition

To further explore the role that groundwater chemistry plays in PFAS adsorption inhibition and to develop a mechanistic interpretation of the data, we constructed a PCA-biplot that describes the relationships between *Inhibition%* (*i.e.*, the height of the bars in Fig. 4) and the major chemical parameters of each groundwater sample in each of the twelve experiments (*i.e.*, three adsorbents, four groundwater samples). The six chemical parameters considered in the PCA analysis were *pH*, *conductivity*, *TOC*, *SUVA*, and the molar concentrations of a variety of *cations* and *anions*. The results of the PCA analysis are provided as Fig. 5.

*pH* exhibited a strong positive correlation with adsorption inhibition (*i.e.,* greater pH values resulted in a greater extent of adsorption inhibition among the anionic PFAS). The anionic PFASs selected for this study have very low $pK_a$ values and are therefore present only as anions within the pH range of the groundwater samples selected for this study. Therefore, the noted pH dependence of *Inhibition%* is more readily explained by changes to the surface charge of the adsorbents rather than to protonation or deprotonation of the adsorbates. AWAC has a negative surface charge in the pH range of 7–8 (Table S4), and the surface charge of AWAC will become increasingly negative at higher pH values. This will lead to greater repulsive electrostatic forces for anionic PFAS at higher pH values, and result in more adsorption inhibition (Deng et al., 2012; Higgins and Luthy, 2006). Both of the CDPs selected for this study have a positive surface charge in the pH range 7–8 (Table S3). However, aCDP contains weakly basic functional groups that will be deprotonated at higher pH values whereas CDP + does not undergo acid-base reactions under these conditions and remains cationic over the studied pH range. The deprotonation of aCDP at higher pH values can weaken (Tang et al., 2010; Zhang et al., 2011a) or eliminate (Yu et al., 2009) the attractive electrostatic interactions between aCDP and anionic PFAS at neutral pH. Our experimental adsorption data suggest that aCDP has a positive surface charge in WA-D but a negative surface charge at the higher pH values measured for GW-A, AA-A, and WA-A; the elimination of the attractive electrostatic interactions between aCDP and anionic PFAS at higher pH values can explain the higher extent of adsorption inhibition in those groundwater samples, and, particularly, the limited *Inhibition%* in WA-D (Fig. 4). The permanently positive charge of CDP + explains the resilience of CDP + to adsorption inhibition in groundwater samples of varying pH, and the relatively low extent of adsorption inhibition observed across all groundwater samples.

The total molar concentration of measured *cations* (*i.e.,* $Ca^{2+}$, $Mg^{2+}$, $K^{+}$, $Na^{+}$) also exhibited a strong positive correlation with adsorption inhibition (*i.e.,* greater concentrations of *cations* resulted in a greater extent of adsorption inhibition among the anionic PFAS). A similar effect has been observed in other studies investigating the adsorption of anionic surfactants on a variety of

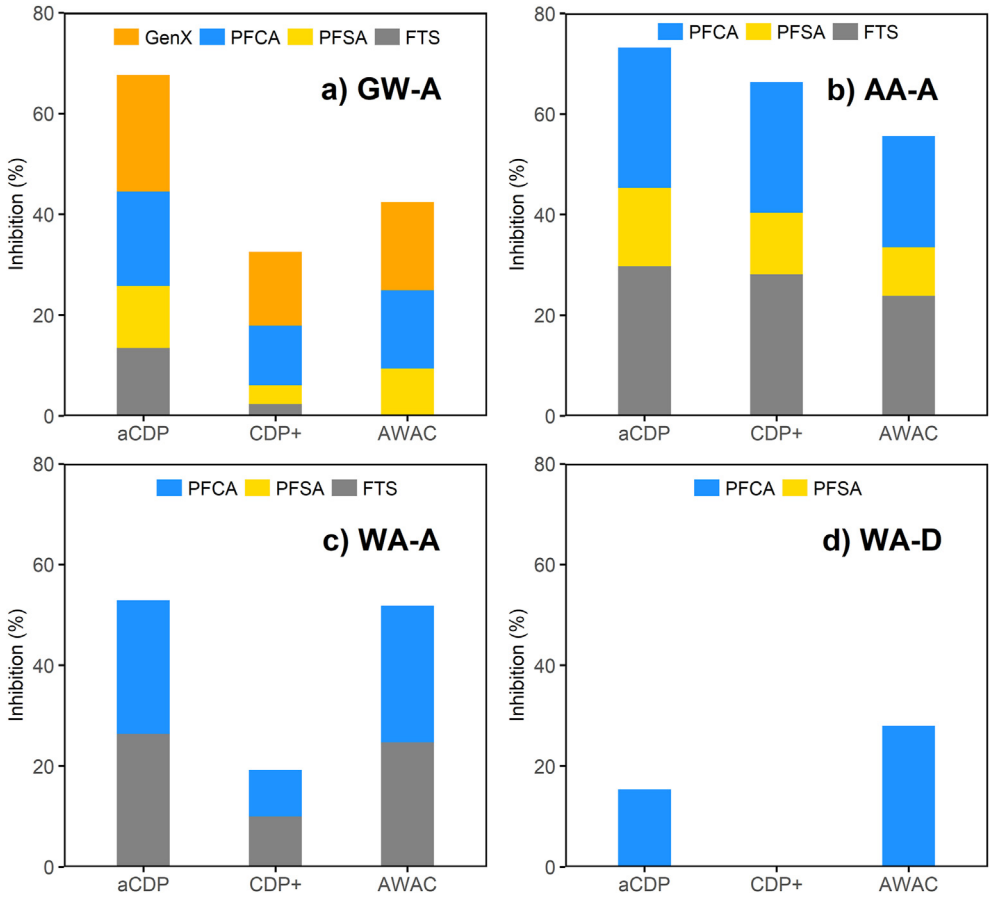


**Fig. 4.** Bar plots exhibiting the adsorption inhibition percentages of 3 adsorbents in 4 groundwater samples at 4h: a) GW-A; b) AA-A; c) WA-A; d) WA-D. The total height of a bar represents the overall percentage of adsorption inhibition (calculated by Equation (5)) a certain adsorbent experienced in a certain groundwater matrix. The fractionated components within each bar represents the relative percentage of decreased adsorption affinity for each class of PFASs comparing to that in Milli-Q water (note that GenX and FTSs were below limits of quantification in specific groundwater samples and thus not labeled in the corresponding legends).

adsorbents (Kwadijk et al., 2013; Wang and Shih, 2011). Previous studies have concluded that divalent cations like $Mg^{2+}$ and $Ca^{2+}$ can bind with the anionic head groups of PFAS to form weak, neutral complexes which can decrease the extent of adsorption by weakening potential electrostatic interactions (Jeon et al., 2011; Wang and Shih, 2011). As is revealed in the PCA-biplot (Fig. 5) and in the raw data (Table S4), groundwater AA-A had the highest concentrations of cations, including divalent cations, among all groundwater samples, which resulted in the greatest extent of adsorption inhibition among all of the adsorbents. This phenomenon also explains the anomalous behavior of CDP+ and AWAC in AA-A noted in the preceding (Fig. 4b). The permanently positive surface charge of CDP+ enhances the removal of anionic PFAS through attractive electrostatic interactions that are diminished in the presence of divalent cations. AWAC has a permanently negative surface charge and relies exclusively on hydrophobic interactions for the adsorption of anionic PFAS and exhibits lower extents of adsorption inhibition in groundwater samples with higher concentrations of divalent cations.

In contrast to the concentration of *cations*, neither *conductivity* nor the concentration of *anions* (*i.e.,* $F^-$, $Cl^-$, $NO_3^-$, $SO_4^{2-}$, $PO_4^{3-}$) exhibited a significant association with adsorption inhibition, indicating that these parameters do not contribute much to the observed adsorption inhibition in this study. Because we have adsorbents that have positive and negative surface charges and adsorbates that are always anionic, this is further evidence that the effect from *cations* is likely due to interactions with the PFAS and not the adsorbent; if *cations* were affecting one type of adsorbent, then we would expect *anions* to affect the adsorbent of the opposite surface charge in an analogous way. Likewise, neither *TOC* nor *SUVA* exhibited a significant association with adsorption inhibition. This finding is notable because dissolved organic matter of a certain size has been previously shown to inhibit adsorption on other types of CDPs (Ling et al., 2020), particularly those that carry a negative surface charge. The lack of an association between *TOC* and *SUVA* and CDP adsorption inhibition in this study suggests that anionic dissolved organic matter may only influence adsorption on negatively charged CDPs.

### 3.5. Implications for practice

Our study sought to explore the potential of conventional and emerging adsorbents to remove anionic PFAS from water, and to identify the factors that lead to adsorption inhibition in groundwater matrices. In WA-D (the un-amended PFAS-contaminated groundwater sample), only CDP + removed PFOA and PFOS to concentrations below the US EPA Health Advisory threshold of 70 ng $L^{-1}$ in our experiments after 4 h of contact time (23 and 24 ng $L^{-1}$, respectively). All three adsorbents (CDP+, aCDP, and AWAC) exhibited limited removal of the shorter-chain carboxylates and sulfonates in WA-D, but CDP + again exhibited the greatest removal of these PFAS in our experiments after 4 h of contact time. In comparing the performance of all adsorbents across experiments conducted in Milli-Q and groundwater, we found that *pH* and the

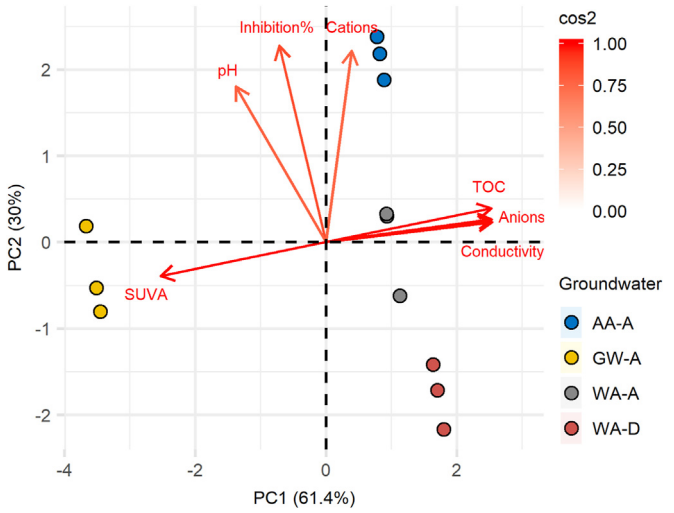


**Fig. 5.** PCA biplot demonstrating the correlations among six groundwater properties and adsorption inhibition (calculated by Equation (5)) at 4h in groundwater matrices. The PCA was established based on a multi-dimensional dataset with 7 variables and 12 observations (three adsorbents by four groundwater matrices). The biplot was plotted against the first two primary components (i.e. PC1 and PC2), which combined to have explained more than 91% of the total variance in the original dataset. The observations were plotted as scattered points and were colored by the groundwater matrix with which they belonged. The variables were plotted as straight arrows, and each variable was colored by its quality of representation (labeled as "cos2" in the legend) on the selected primary components (a lighter color indicates that the variable contributed less to the primary components). The correlations between variables were manifested by the angles in between the arrows. The magnitude an observation had for a certain variable was revealed by the point's position relative to the direction of the arrow (if the point locates in the same direction that an arrow is pointing at, the observation has a higher magnitude of this chosen variable). (For interpretation of the references to color in this figure legend, the reader is referred to the Web version of this article.)

presence of inorganic *cations* contribute to adsorption inhibition to varying extents, depending on the adsorbent. These data could be used to help guide the selection of remediation technologies based on local environmental conditions. Together, the new insights developed in our analyses improve our understanding of PFAS-adsorbent interactions and will lead to the continued development of novel adsorbents targeting a broad family of PFASs and the design of more effective water treatment processes for PFAS-contaminated systems.

## 4. Conclusions

- The adsorption behaviors of 20 target PFASs (including 4 classes containing members with varying chain lengths) onto 5 types of adsorbents (including 3 ACs and 2 CDPs) were studied in Milli-Q water. ACs of larger particle size exhibited slower removal kinetics, likely due to intra-particle diffusion limitations. Additionally, PFASs of shorter chain length were observed to have faster initial adsorption onto the larger-sized ACs, further indicating the probable steric-related resistance that larger PFAS molecules may experience when transporting within the micropores of ACs. In comparison, all smaller-sized ACs and the two CDPs exhibited nearly complete removal of the target PFASs and seemed to be unaffected by intra-particle diffusion limitations.
- There was a clear trend that PFAS removal can be greatly improved in kinetics, if not in capacity, with a decrease in the AC *particle size*. A PCA-biplot was constructed to further explore the effect of *particle size*, and the results suggested that, although there were differences in surface charge and pore volume distributions among different types of ACs, none of these variables exhibited a significant association with the PFAS removal performance. Consequently, the *particle size* exhibited a significant association and we attribute that finding to an increased specific external surface area or the generation of more active binding sites that were originally inaccessible.
- Based on the adsorption performance in Milli-Q water, three adsorbents (AWAC, aCDP, CDP+) were selected for further experimentation in groundwater. Although all three adsorbents demonstrated nearly ideal performance in Milli-Q water, their PFAS uptake in the groundwater experiments were all inhibited, and were inhibited to different degrees, implying that every adsorbent had its own unique mechanism in removing the target PFASs and in interacting with the groundwater matrices. Regardless of the adsorbent type, the uptake of PFSAs were impacted the least compared to all other PFASs, indicating a higher adsorption affinity for this group of PFAS molecules.
- An approach to quantify the extent of adsorption inhibition was introduced and PCA-biplots were constructed to investigate the role that certain groundwater matrix constituents play in adsorption inhibition. *pH* and the concentration of *cations* exhibited positive associations to adsorption inhibition. Given that the varying pH should have a limited effect on the strongly acidic PFAS anions, adsorption inhibition by means of alterations of the adsorbent surface chemistry was proposed. The influence of *cations* was particularly prominent in the AA-A groundwater for CDP+, indicating that the increased concentration of divalent cations in AA-A might have weakened the electrostatic attractions between the PFAS anions and the positively charged CDP+.

## Declaration of competing interest

The authors declare the following financial interests/personal relationships which may be considered as potential competing interests:

Cornell University has filed US and international patent applications related to the porous cyclodextrin polymer studied in this manuscript. W.R.D. and D.E.H. serve on the scientific advisory board and have equity and/or stock purchase options in CycloPure, Inc., which is commercializing related porous cyclodextrin polymers and partially funded this study.

## Acknowledgements

This work was supported by a grant from CycloPure, Inc., (D.E.H.), the NSF Center for Sustainable Polymers, CHE - 1901635 (W.R.D.), and the Strategic Environmental Research and Development Program, ER18-1026 (D.E.H. and W.R.D.).

## Appendix A. Supplementary data

Supplementary data to this article can be found online at https://doi.org/10.1016/j.watres.2020.115950.

## References

Ahrens, L., Taniyasu, S., Yeung, L.W., Yamashita, N., Lam, P.K., Ebinghaus, R., 2010. Distribution of polyfluoroalkyl compounds in water, suspended particulate matter and sediment from Tokyo Bay, Japan. Chemosphere 79 (3), 266–272.

Ando, N., Matsui, Y., Kurotobi, R., Nakano, Y., Matsushita, T., Ohno, K., 2010. Comparison of natural organic matter adsorption capacities of super-powdered activated carbon and powdered activated Carbon. Water Res. 44 (14), 4127–4136.

Arias Espana, V.A., Mallavarapu, M., Naidu, R., 2015. Treatment technologies for aqueous perfluorooctanesulfonate (PFOS) and perfluorooctanoate (PFOA): a critical review with an emphasis on field testing. Environ. Technol. Innov. 4, 168–181.

Ateia, M., Arifuzzaman, M., Pellizzeri, S., Attia, M.F., Tharayil, N., Anker, J.N., Karanfil, T., 2019. Cationic polymer for selective removal of GenX and short-

chain PFAS from surface waters and wastewaters at ng/L levels. Water Res. 163, 114874.
Chen, W., Zhang, X., Mamadiev, M., Wang, Z., 2017. Sorption of perfluorooctane sulfonate and perfluorooctanoate on polyacrylonitrile fiber-derived activated carbon fibers: in comparison with activated carbon. RSC Adv. 7 (2), 927–938.
Deng, S., Zhang, Q., Nie, Y., Wei, H., Wang, B., Huang, J., Yu, G., Xing, B., 2012. Sorption mechanisms of perfluorinated compounds on carbon nanotubes. Environ. Pollut. 168, 138–144.
Domingo, J.L., Nadal, M., 2019. Human exposure to per- and polyfluoroalkyl substances (PFAS) through drinking water: a review of the recent scientific literature. Environ. Res. 177, 108648.
Eschauzier, C., Beerendonk, E., Scholte-Veenendaal, P., De Voogt, P., 2012. Impact of treatment processes on the removal of perfluoroalkyl acids from the drinking water production chain. Environ. Sci. Technol. 46 (3), 1708–1715.
Guelfo, J.L., Marlow, T., Klein, D.M., Savitz, D.A., Frickel, S., Crimi, M., Suuberg, E.M., 2018. Evaluation and management strategies for per- and polyfluoroalkyl substances (PFASs) in drinking water aquifers: perspectives from impacted U.S. Northeast communities. Environ. Health Perspect. 126 (6), 065001.
Hansen, M.C., Børresen, M.H., Schlabach, M., Cornelissen, G., 2010. Sorption of perfluorinated compounds from contaminated water to activated carbon. J. Soils Sediments 10 (2), 179–185.
Hatton, J., Holton, C., DiGuiseppi, B., 2018. Occurrence and behavior of per- and polyfluoroalkyl substances from aqueous film-forming foam in groundwater systems. Remed. J. 28 (2), 89–99.
Higgins, C.P., Luthy, R.G., 2006. Sorption of perfluorinated surfactants on sediments. Environ. Sci. Technol. 40 (23), 7251–7256.
Houtz, E., Wang, M., Park, J.S., 2018. Identification and fate of aqueous film forming foam derived per- and polyfluoroalkyl substances in a wastewater treatment plant. Environ. Sci. Technol. 52 (22), 13212–13221.
Inyang, M., Dickenson, E.R.V., 2017. The use of carbon adsorbents for the removal of perfluoroalkyl acids from potable reuse systems. Chemosphere 184, 168–175.
Jeon, J., Kannan, K., Lim, B.J., An, K.G., Kim, S.D., 2011. Effects of salinity and organic matter on the partitioning of perfluoroalkyl acid (PFAs) to clay particles. J. Environ. Monit. 13 (6), 1803–1810.
Karoyo, A.H., Borisov, A.S., Wilson, L.D., Hazendonk, P., 2011. Formation of host-guest complexes of beta-cyclodextrin and perfluorooctanoic acid. J. Phys. Chem. B 115 (31), 9511–9527.
Karoyo, A.H., Wilson, L.D., 2013. Tunable macromolecular-based materials for the adsorption of perfluorooctanoic and octanoic acid anions. J. Colloid Interface Sci. 402, 196–203.
Klemes, M.J., Ling, Y., Ching, C., Wu, C., Xiao, L., Helbling, D.E., Dichtel, W.R., 2019. Reduction of a tetrafluoroterephthalonitrile-β-cyclodextrin polymer to remove anionic micropollutants and perfluorinated alkyl substances from water. Angew. Chem. Int. Ed. 58 (35), 12049–12053.
Kwadijk, C.J., Velzeboer, I., Koelmans, A.A., 2013. Sorption of perfluorooctane sulfonate to carbon nanotubes in aquatic sediments. Chemosphere 90 (5), 1631–1636.
Ling, Y., Alzate-Sánchez, D.M., Klemes, M.J., Dichtel, W.R., Helbling, D.E., 2020. Evaluating the effects of water matrix constituents on micropollutant removal by activated carbon and β-cyclodextrin polymer adsorbents. Water Res. https://doi.org/10.1016/j.watres.2020.115551.
Martin, D., Munoz, G., Mejia-Avendano, S., Duy, S.V., Yao, Y., Volchek, K., Brown, C.E., Liu, J., Sauve, S., 2019. Zwitterionic, cationic, and anionic perfluoroalkyl and polyfluoroalkyl substances integrated into total oxidizable precursor assay of contaminated groundwater. Talanta 195, 533–542.
McCleaf, P., Englund, S., Ostlund, A., Lindegren, K., Wiberg, K., Ahrens, L., 2017. Removal efficiency of multiple poly- and perfluoroalkyl substances (PFASs) in drinking water using granular activated carbon (GAC) and anion exchange (AE) column tests. Water Res. 120, 77–87.
Merino, N., Qu, Y., Deeb, R.A., Hawley, E.L., Hoffmann, M.R., Mahendra, S., 2016. Degradation and removal methods for perfluoroalkyl and polyfluoroalkyl substances in water. Environ. Eng. Sci. 33 (9), 615–649.
Mostert, M.M.R., Ayoko, G.A., Kokot, S., 2010. Application of chemometrics to analysis of soil pollutants. Trac. Trends Anal. Chem. 29 (5), 430–445.
Murray, C.C., Vatankhah, H., McDonough, C.A., Nickerson, A., Hedtke, T.T., Cath, T.Y., Higgins, C.P., Bellona, C.L., 2019. Removal of per- and polyfluoroalkyl substances using super-fine powder activated carbon and ceramic membrane filtration. J. Hazard Mater. 366, 160–168.
Nassi, M., Sarti, E., Pasti, L., Martucci, A., Marchetti, N., Cavazzini, A., Di Renzo, F., Galarneau, A., 2014. Removal of perfluorooctanoic acid from water by adsorption on high surface area mesoporous materials. J. Porous Mater. 21 (4), 423–432.
Partlan, E., Davis, K., Ren, Y., Apul, O.G., Mefford, O.T., Karanfil, T., Ladner, D.A., 2016. Effect of bead milling on chemical and physical characteristics of activated carbons pulverized to superfine sizes. Water Res. 89, 161–170.
Pérez-Arribas, L.V., León-González, M.E., Rosales-Conrado, N., 2017. Learning principal component analysis by using data from air quality networks. J. Chem. Educ. 94 (4), 458–464.
Piai, L., Dykstra, J., Adishakti, M.G., Blokland, M., Langenhoff, A., van der Wal, A., 2019. Diffusion of hydrophilic organic micropollutants in granular activated carbon with different pore sizes. Water Res. 162, 518–527.
Punyapalakul, P., Suksomboon, K., Prarat, P., Khaodhiar, S., 2013. Effects of surface functional groups and porous structures on adsorption and recovery of perfluorinated compounds by inorganic porous silicas. Separ. Sci. Technol. 48 (5), 775–788.
Rahman, M.F., Peldszus, S., Anderson, W.B., 2014. Behaviour and fate of perfluoroalkyl and polyfluoroalkyl substances (PFASs) in drinking water treatment: a review. Water Res. 50, 318–340.
Schultes, L., Peaslee, G.F., Brockman, J.D., Majumdar, A., McGuinness, S.R., Wilkinson, J.T., Sandblom, O., Ngwenyama, R.A., Benskin, J.P., 2019. Total fluorine measurements in food packaging: how do current methods perform? Environ. Sci. Technol. Lett. 6 (2), 73–78.
Tang, C.Y., Shiang Fu, Q., Gao, D., Criddle, C.S., Leckie, J.O., 2010. Effect of solution chemistry on the adsorption of perfluorooctane sulfonate onto mineral surfaces. Water Res. 44 (8), 2654–2662.
Tang, P., Sun, Q., Zhao, L., Tang, Y., Liu, Y., Pu, H., Gan, N., Liu, Y., Li, H., 2019. A simple and green method to construct cyclodextrin polymer for the effective and simultaneous estrogen pollutant and metal removal. Chem. Eng. J. 366, 598–607.
Wang, F., Shih, K., 2011. Adsorption of perfluorooctanesulfonate (PFOS) and perfluorooctanoate (PFOA) on alumina: influence of solution pH and cations. Water Res. 45 (9), 2925–2930.
Wang, W., Maimaiti, A., Shi, H., Wu, R., Wang, R., Li, Z., Qi, D., Yu, G., Deng, S., 2019. Adsorption behavior and mechanism of emerging perfluoro-2-propoxypropanoic acid (GenX) on activated carbons and resins. Chem. Eng. J. 364, 132–138.
Weiss-Errico, M.J., O'Shea, K.E., 2017. Detailed NMR investigation of cyclodextrin-perfluorinated surfactant interactions in aqueous media. J. Hazard Mater. 329, 57–65.
Xiao, L., Ling, Y., Alsbaiee, A., Li, C., Helbling, D.E., Dichtel, W.R., 2017a. Beta-cyclodextrin polymer network sequesters perfluorooctanoic acid at environmentally relevant concentrations. J. Am. Chem. Soc. 139 (23), 7689–7692.
Xiao, X., Ulrich, B.A., Chen, B., Higgins, C.P., 2017b. Sorption of poly- and perfluoroalkyl substances (PFASs) relevant to aqueous film-forming foam (AFFF)-Impacted groundwater by biochars and activated carbon. Environ. Sci. Technol. 51 (11), 6342–6351.
Yu, Q., Zhang, R., Deng, S., Huang, J., Yu, G., 2009. Sorption of perfluorooctane sulfonate and perfluorooctanoate on activated carbons and resin: kinetic and isotherm study. Water Res. 43 (4), 1150–1158.
Zhang, D., Luo, Q., Gao, B., Chiang, S.Y., Woodward, D., Huang, Q., 2016. Sorption of perfluorooctanoic acid, perfluorooctane sulfonate and perfluoroheptanoic acid on granular activated carbon. Chemosphere 144, 2336–2342.
Zhang, Q., Deng, S., Yu, G., Huang, J., 2011a. Removal of perfluorooctane sulfonate from aqueous solution by crosslinked chitosan beads: sorption kinetics and uptake mechanism. Bioresour. Technol. 102 (3), 2265–2271.
Zhang, X., Niu, H., Pan, Y., Shi, Y., Cai, Y., 2011b. Modifying the surface of Fe3O4/SiO2 magnetic nanoparticles with C18/NH2 mixed group to get an efficient sorbent for anionic organic pollutants. J. Colloid Interface Sci. 362 (1), 107–112.
Zhao, D., Cheng, J., Vecitis, C.D., Hoffmann, M.R., 2011. Sorption of perfluorochemicals to granular activated carbon in the presence of ultrasound. J. Phys. Chem. 115 (11), 2250–2257.